Proceedings of the 3rd Marine Energy Technology Symposium
METS2015
April 27-29, 2015, Washington, DC

PREDICTING TIDAL CURRENT TURBINE PERFORMANCE IN BLOCKED OPERATING CONDITIONS

Christopher Vogel*
University of Oxford
Oxford, United Kingdom

Richard Willden
University of Oxford
Oxford, United Kingdom

Guy Houlsby
University of Oxford
Oxford, United Kingdom

ABSTRACT

The renewable tidal current resource has attracted significant global interest as a predictable energy resource. Although the understanding of the tidal current resource has advanced considerably by transferring knowledge from the wind energy industry, a number of important differences exist between wind and tidal current turbines. Chief among these differences is that inter-turbine spacing in the constrained flow fields in which tidal current turbines operate has a significant effect on the power that may be extracted from the flow, as the turbines are able to operate at higher thrust levels than wind turbines. Exploiting this advantage requires that tidal current turbines are designed to achieve the required thrusts, and this paper adapts another tool that has been widely used in the wind turbine industry, blade element momentum (BEM) theory, to incorporate the effects of blockage, in order to investigate the effects on tidal current turbine design and performance. The blockage corrected BEM tool can also be used to investigate turbine performance when rated power is achieved, as simplified actuator disc models are presently unable to investigate turbine performance in such conditions. Together, these provide useful information to device developers when designing turbines for deployment in closely-packed arrays.

INTRODUCTION

Tidal current energy has attracted increasing worldwide attention as a predictable renewable energy resource. Many different device designs exist, and many techniques have been borrowed from the analysis of wind turbines in order to better understand the potential of tidal current turbines. Amongst these is linear momentum actuator disc theory, originally employed by Lanchester [1] and Betz [2] to show that the peak power coefficient of an actuator disc representing a wind turbine was 0.593. This theory was adapted by Garrett and Cummins [3] for tidal current turbines where they analysed an actuator disc in a flow passage with a rigid lid. The concept of blockage, B, (ratio of device frontal area to flow passage cross-sectional area) was employed, and it was shown that the maximum power coefficient increases as $(1-B)^{-2}$ above the Lanchester-Betz limit.

Nishino and Willden [4] showed that effect of blockage is important both at the device and array scales, and a significant increase in performance may be achieved by placing actuator discs closely together even when only a small fraction of the channel cross-section is occupied. Power is increased in high blockage configurations as the increased blockage (and hence reduced area for the flow to bypass the turbines) means that it is possible to exert a higher thrust on the flow for a given flow speed through the turbines. Although realistic turbines will not be able to fully achieve the power predicted for actuator discs, turbines may be designed to be capable of exerting the levels of thrust required to achieve a significant fraction of these predictions. Blade Element Momentum (BEM) theory is a widely used design tool in the wind turbine industry, and its use in tidal current turbine design requires blockage effects to be incorporated within the design routine, which shall be discussed in this paper.

A particular challenge facing device developers is the fluctuation of the tidal stream resource in accordance with the locally dominant tidal constituents, as this has a significant impact on the economic feasibility and hence design of tidal stream turbines. Some fluctuations may occur over a period of hours in response to the diurnal and semi-diurnal constituents, whereas others, such as the spring-neap tidal cycle, occur over longer time periods. The temporal variation in the strength of tidal currents means that it may not economically feasible to design tidal

*Corresponding Author: christopher.vogel@eng.ox.ac.uk

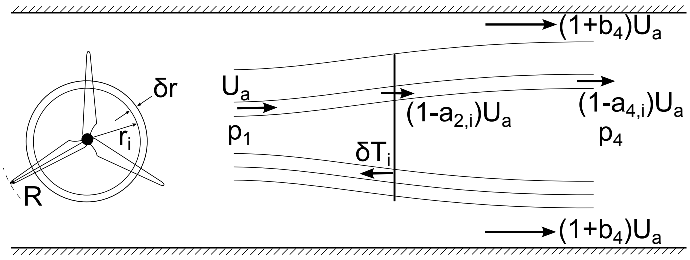

FIGURE 1. Diagram of the blockage corrected BEM model. Station one is far upstream of the rotor plane, station two is at the rotor plane, and station four is far downstream of the turbine plane, where the static pressure equalises across the core and bypass flows.

devices to extract the peak power available in a tidal basin or channel, as the devices will operate significantly below their capacity for large fraction of the tidal cycle. Instead, devices will be designed to achieve a rated power at a given flow speed which optimises the ratio of the revenue from the power extracted to the cost of the turbine and generator. Turbine thrust may consequently vary with flow speed differently above and below the rated flow speed in order to maintain rated power, which in turn will affect the interaction between turbines and the tidal resource. Such interactions need to be understood in order to accurately assess the power that may be extracted by tidal turbine arrays and the subsequent effect on the environment.

This paper will contain two main sections; the first develops a blockage-corrected blade element momentum theory, and the second applies the adapted BEM model to investigate turbine performance in power capping conditions.

BLOCKAGE CORRECTED BLADE ELEMENT MOMENTUM THEORY

A wind turbine is generally modelled as operating in an unblocked flow in which there is a full recovery of the static pressure far downstream of the rotor. The removal of momentum from a volume-flux constrained flow by a tidal turbine however results in a static pressure deficit in the far wake of the rotor due to continuity requirements, and hence a static pressure gradient is established in the flow passage, as illustrated in Figure 1. The static pressure gradient results in a greater pressure gradient across the rotor plane for a given thrust in the blocked flow than in the unblocked flow. There is hence a greater flow speed through the rotor plane of the blocked rotor, which generally results in increased torque and therefore power, depending on the angle of attack of the rotor blades. The flow speed through the rotor plane and in the far wake depends on the applied thrust and the blockage ratio, and consequently, the simple relationship in standard BEM theory in which the velocity deficit in the far wake is twice the velocity deficit at the rotor plane no longer holds, necessitating the development of a more generalised BEM model, or embedding the BEM model within a computational domain in order to account for the accelerated flow (for examples, see [5], [6], [7]). However, such simulations require moderate computational expense which is detrimental when designing turbines, and it would be advantageous to instead have a blockage-corrected BEM tool. The changes to the momentum equations in BEM theory due to the static pressure gradient are outlined herein. A detailed account of standard BEM theory for comparison may be found in [8].

The upstream boundary of the finite blockage BEM model is derived from the larger-scale flow around the turbine, which may, for example, be the flow through an array of turbines. This provides the upstream flow speed, u_a, which is taken as the reference velocity for the turbine-scale model, as shown in Figure 1. The flow through the rotor is divided into N independent annular stream tubes, which are encompassed by the bypass flow. The downstream boundary of the finite blockage BEM model is the point at which the static pressure equalises across the annular stream tubes and the bypass flow, although the possibility of differing flow speeds is allowed. The inductions factors for the velocity $u_{2d,i}$ through the i^{th} streamtube through the rotor, $a_{2,i}$ and the velocity $u_{4d,i}$ in the wake of the turbine, $a_{4,i}$, are defined relative to the reference flow speed u_a:

$$u_{2d,i} = (1-a_{2,i})u_a; \qquad u_{4d,i} = (1-a_{4,i})u_a. \tag{1}$$

Likewise, the induction factor for the bypass velocity u_{4b} at the static pressure equalisation point is defined relative to the reference velocity as:

$$u_{4b} = (1+b_4)u_a. \tag{2}$$

Blockage Corrected BEM Model

Conservation of mass and momentum are considered in the annular streamtubes, the i^{th} annular streamtube being at radius r_i from the centre of rotation and having a thickness of δr_i. Conservation of momentum in the i^{th} annular ring upstream and downstream of the rotor plane yields an expression for the incremental thrust δT_i:

$$\delta T_i = \rho \pi r_i u_a^2 \left(b_4^2 + 2b_4 + 2(1-a_{2,i})a_{4,i}\right)\delta r_i. \tag{3}$$

The incremental thrust may also be written as the sum of the lift and drag on the i^{th} blade element. The flow angle between the relative velocity $u_{rel,i}$ and the direction of rotation is defined as $\phi_i = \alpha_i + \beta_i$, where α_i is the angle of attack and β_i is the blade twist angle on the elemental section. Defining the number of rotor blades as N_B and the blade element chord length to be c_i, this gives:

$$\delta T_i = \frac{1}{2}\rho u_{rel,i}^2 N_B c_i \left(C_{l,i}\cos\phi_i + C_{d,i}\sin\phi_i\right)\delta r_i, \tag{4}$$

where $C_{l,i}$ and $C_{d,i}$ are the sectional lift and drag coefficients of the blade element respectively. Equating (3) and (4), an expression for $a_{4,i}$ is found:

$$a_{4,i} = \frac{\sigma_i(1-a_{2,i})^2\left(C_{l,i}\cos\phi_i + C_{d,i}\sin\phi_i\right) - b_4(2+b_4)\sin^2\phi_i}{2(1-a_{2,i})\sin^2\phi_i}, \tag{5}$$

where $\sigma_i = \frac{N_B c_i}{2\pi r_i}$ is the solidity of the i^{th} annular ring.

The angular velocity of the rotor blades is Ω, and an angular velocity factor a_i' is induced in the i_{th} annular ring at the rotor plane. The incremental torque, δQ_i, on the i^{th} annular ring can be found in a similar manner to the incremental thrust by considering conversation of angular momentum in an annular ring:

$$\delta Q_i = 4\pi\rho r_i^3 u_a(1-2a_{2,i})\Omega a_i'\delta r_i. \tag{6}$$

The torque may also be expressed in terms of the forces on the blade element as:

$$\delta Q_i = \frac{1}{2}\rho u_{rel,i}^2 N_B c_i r_i \left(C_{l,i}\sin\phi_i - C_{d,i}\cos\phi_i\right)\delta r_i. \tag{7}$$

Eliminating δQ_i between (6) and (7) yields an expression for the annular induction factor:

$$a_i' = \frac{\sigma_i\left(C_{l,i}\sin\phi_i - C_{d,i}\cos\phi_i\right)}{4\sin\phi_i\cos\phi_i - \sigma_i\left(C_{l,i}\sin\phi_i - C_{d,i}\cos\phi_i\right)}. \tag{8}$$

The system of equations is closed using linear momentum actuator disc theory as presented in [3]. Equation 2.22 in the rigid lid LMADT model in [3] may be rearranged for a quadratic in the wake induction factor a_4:

$$(1-B)(1+b_4)^2 + B(1-a_{4,i})^2 - 2a_{4,i}b_4 - 1 = 0, \tag{9}$$

which may be solved to give $a_{4,i}$:

$$a_{4,i} = 1 + \frac{b_4 - \sqrt{(1-B)b_4^2 + B^2(1+b_4)^2}}{B}. \tag{10}$$

This is combined with the expression for thrust in Equation 2.8 in [3]:

$$\delta T_i = \rho\pi r_i u_a^2\left(b_4^2 + 2(a_{4,i}+b_4) - a_{4,i}^2\right)\delta r_i, \tag{11}$$

which is summed over the annuli to give a quartic equation for b_4 in terms of the aggregate turbine thrust, blockage ratio, turbine area, and the reference velocity. The solution to the quartic equation determines the value of b_4 that is consistent with the pressure gradient that develops in the flow passage due to the thrust applied to the flow, which can then be used to close the system of equations defining the blockage-corrected BEM model.

This blockage-corrected BEM problem is solved given the specification of the rotor's blockage ratio B, tip speed ratio, λ, and rotor data, such as lift and drag curves with respect to angle of attack, blade twist and solidity data, and the flow conditions. The solution procedure of the blockage-corrected BEM follows the standard iterative procedure to solve BEM theory for a wind turbine, such as that presented in [8], with the modified equations presented above. Initial estimates of b_4 and ϕ_i allow $a_{4,i}$ in (5) and a_i' in (8) to be determined, which are then used to update the estimates of the angle of incidence ϕ_i:

$$\tan\phi_i = \frac{u_a(1-a_{2,i})}{r_i\Omega(1+a_i')}, \tag{12}$$

and b_4 is re-evaluated using LMADT based on the aggregate thrust applied to the flow. The system of equations is solved iteratively until convergence to a relative error of 10^{-6} is achieved.

BEM analysis usually assumes that fluid particles passing through the swept area of each rotor annulus undergo the same loss of momentum, which assumes that the rotor has sufficiently many blades to ensure that all fluid particles interact with a blade as they pass through the rotor plane. Corrections exist to account for the effects of a finite number of blades on the rotor performance, such as the Prandtl tip loss model, which reduces the axial induction factor $a_{2,i}$ to zero as the rotor tip is approached, and has been implemented here:

$$F_i = \frac{2}{\pi}\arccos e^{-f_i}, \qquad f_i = \frac{N_B}{2}\frac{R-r_i}{r_i\sin\phi_i}. \tag{13}$$

It is presently unclear whether the Prandtl tip loss model best describes the flow conditions near the tips of tidal turbine rotor blades, as the effect of the volume flux constraint on the interaction with the free stream flow and the rotor tips is currently unknown. However, the Prandtl tip loss model represents one of the most widely accepted models for wind turbines, and hence offers a useful basis from which additional research may be undertaken.

Comparison to Numerical Simulation

Performance of the blockage-corrected BEM model is investigated by comparison to numerical investigation of a two-bladed, 5m diameter rotor based on the Risø-A1-24 aerofoil

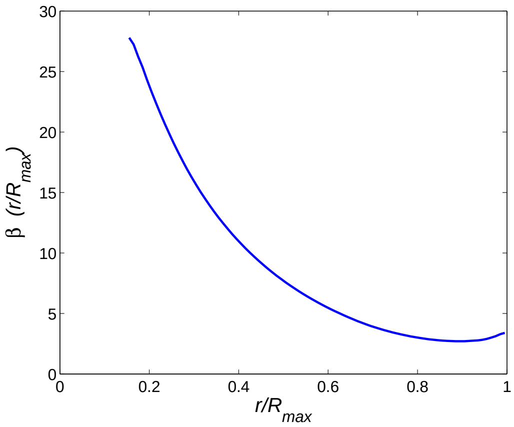

FIGURE 2. Radial variation of blade twist angle β of rotor design from [6].

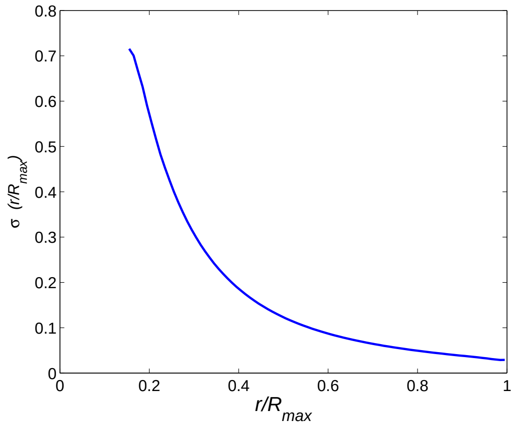

FIGURE 3. Radial variation of solidity ratio σ of rotor design from [6].

optimised by Schluntz [6] for an unblocked flow and tested in blocked conditions. The design achieves a peak C_P of 0.49 at a tip speed ratio λ of 5. The optimised blade twist angle β and solidity ratio σ are shown in Figures 2 and 3 respectively.

Garrett and Cummins' rigid lid actuator disc theory predicts that the maximum power coefficient should increase when the blockage ratio increases from 0. Figure 4 compares the power coefficient and tip speed ratio curves for the unblocked turbine design in unblocked and blocked conditions, where the blockage ratio $B = 0.2$ in the latter case. The peak power coefficient increases to $C_P = 0.63$, and occurs at a higher tip speed ratio of $\lambda = 5.5$. This is because the cross-stream and vertical flow boundaries cause a pressure gradient to form in the flow in response to the applied thrust. The streamwise pressure change results in a higher power being achieved by the turbine as a higher

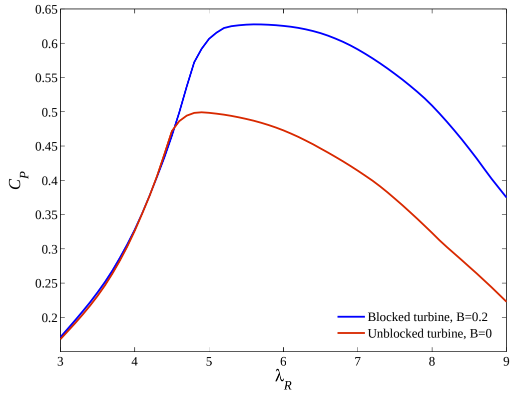

FIGURE 4. Comparison of C_P vs. λ for the unblocked turbine (red) and the same turbine in a blocked channel $B = 0.2$ (blue).

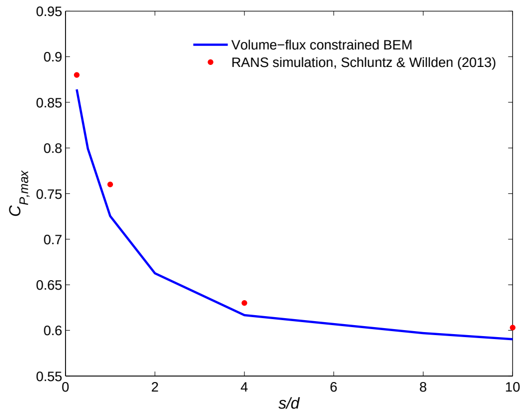

FIGURE 5. Comparison of volume-flux constrained BEM maximum power coefficient (blue) and maximum power coefficient from numerical simulations by [6] (red).

flow speed is maintained through the turbine, which in turn also increases the tip speed ratio. A consequence of the higher peak power coefficient is that a blocked rotor achieves rated power at a lower flow speed than an unblocked turbine, which may improve performance statistics when power capping is implemented.

Figure 5 compares the blockage-corrected BEM model to the numerical simulations conducted by Schluntz [6] for the same turbine in a range of inter-turbine spacing ratios (where $s/_d$ is the turbine tip-to-tip spacing ratio and the water depth is $2d$). The figure shows the maximum power coefficient achieved with respect to the tip-speed ratio at each lateral spacing considered. The volume-flux constrained model agrees well with the numerical simulations. The volume-flux constrained BEM model slightly underestimates the maximum power coefficient determined from the numerical simulations as the expansion of

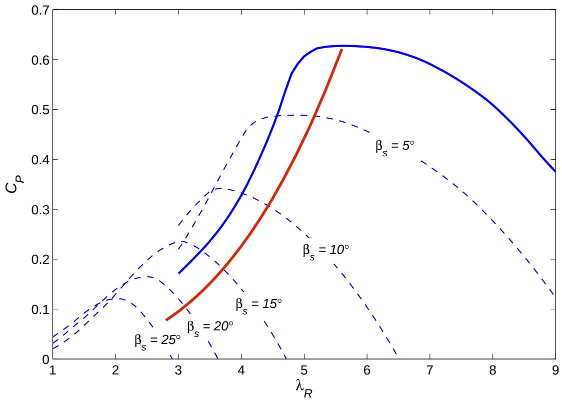

FIGURE 6. Power coefficient C_P vs. tip speed ratio λ for pitch-to-feather increments of 5○ (design curve in solid blue line, dashed blue lines for feathered blades). The target C_P vs. λ curve for power capping is shown in red.

the wake in numerical simulations enhances the blockage of the flow, slightly increasing the flow speed through the turbine and thus the power.

TURBINE PERFORMANCE DURING POWER CAPPING

Many methods have been proposed for maintaining rated power once the rated flow speed is exceeded by the turbine, however, the ultimate result is to reduce the turbine power coefficient as flow speed increases in order to maintain the same overall level of power. Introducing the ratio $\gamma = \frac{u}{u_r}$, where u is the flow speed and the subscript r indicates the rated flow speed, the power coefficient must change as:

$$C_P = \frac{P_r}{\frac{1}{2}\rho u_r^3 A_D} \frac{1}{\gamma^3}, \tag{14}$$

where P_r is the rated power and A_D is the rotor swept area. One commonly adopted method for reducing the rotor power is to adjust the blade pitch to change the lift/drag ratio of the hydrofoil. This paper investigates the effect of feathering the rotor blades to reduce the thrust, and hence the power, of the turbine. It is assumed that the tip speed ratio reduces in order to maintain the rotor's rotational speed, as the blades would otherwise experience cavitation as the blade pitch increased to high values, and consequently the tip speed ratio must follow:

$$\lambda = \frac{R\Omega_r}{u} = \lambda_r \frac{1}{\gamma}. \tag{15}$$

Equations (14) and (15) parameterise a curve that the blocked rotor could follow in order to maintain rated power when the rated flow speed is exceeded, and is shown in red in Figure 6. C_P vs. λ curves are shown for blade pitch angles increasing in 5° increments from the design (solid blue) configuration in dashed blue lines, where it can be seen that the rotor pitch increases by about 23° before the rotor would cut out. The rotor operates at the upper right end of the red line, corresponding to the peak power coefficient, until rated power is achieved, at which point it would begin to traverse the red line down towards the bottom left in order to maintain rated power. In the full paper, it will be shown that this results in a reduction in turbine thrust, which reduces the effect of power extraction by the turbines on the natural flow in the channel. Alternative mechanisms for controlling the power coefficient are also investigated, and the consequences on the flow in a tidal channel between two large bodies of water is investigated using shallow water simulations in TELEMAC-2D.

ACKNOWLEDGMENT

The authors would like to acknowledge the financial support of the Oxford Martin School in this research. The authors would also like to thank J. Schluntz for providing numerical data for comparison to the present work.

REFERENCES

[1] Lanchester, F., 1915. "A contribution to the theory of propulsion and the screw propeller". *Transactions of the Institute of Naval Architects*, ***57***, pp. 98–116.

[2] Betz, A., 1920. "Das Maximum der theoretisch moglichen Ausnutzung des Windes durch Windmotoren". *Zeitschrift für das gesamte Turbinenwesen*, ***26***, pp. 307–309.

[3] Garrett, C., and Cummins, P., 2007. "The efficiency of a turbine in a tidal channel". *Journal of Fluid Mechanics*, ***508***, pp. 243–251.

[4] Nishino, T., and Willden, R., 2012. "The efficiency of an array of tidal turbines partially blocking a wide channel". *Journal of Fluid Mechanics*, ***708***, pp. 596–606.

[5] Masters, I., Chapman, J. C., Willis, M. R., and Orme, J. A. C., 2011. "A robust blade element momentum theory model for tidal stream turbines including tip and hub loss corrections". *Journal of Marine Engineering and Technology*, ***10***(1), pp. 25–35.

[6] Schluntz, J., 2014. Tidal turbine array modelling. DPhil thesis, University of Oxford.

[7] Edmunds, M., Malki, R., Williams, A. J., Masters, I., and Croft, T. N., 2014. "Aspects of tidal stream turbine modelling in the natural environment using a coupled BEM-CFD model". *International Journal of Marine Energy*, ***7***, pp. 20–42.

[8] Burton, T., Sharpe, D., Jenkins, N., and Bossanyi, E., 2001. *Wind Energy Handbook*. West Sussex: John Wiley & Sons, Ltd.